

# Speed-Sensorless DFIG Wind Turbine for Power Optimization Using Fuzzy Sliding Mode Observer

Gadouche Zoubir\*‡, BELFEDAL Cheikh \*, ALLAOUI Tayeb\*, Belabbas belkacem\*

\*Department of Electrical Engineering, L2GEGI Laboratory, IBN KHALDOUN University, Tiaret , Algeria

(zoubir.gadouche@univ-tiaret.dz, bochradz@yahoo.com, allaoui\_tb@yahoo.fr, belabbas.belkacem@univ-tiaret.dz)

‡Corresponding Author; Gadouche Zoubir, Department of Electrical Engineering, L2GEGI Laboratory, IBN KHALDOUN University, Tiaret, Algeria, Tel: +213 778 411 302, zoubir.gadouche@univ-tiaret.dz

*Received: 02.11.2016 Accepted:10.12.2016*

**Abstract-** In practice, speed erroneous measurements in the wind or in the rotor turbine generator, necessarily lead to non-optimal power transmission. This paper presents optimal power control of DWECS (DFIG-based wind energy conversion system), without mechanical speed sensor. In this context, we are interested to develop a speed FSMO (fuzzy sliding mode observer), in order to estimate the DFIG speed. The proposed method linked an indirect power control (IPC) and MPPT without speed subservience and FSMO to assess the rotor speed, for the wind turbine generator Power Control. The results presented are, a comparative study between SMO and FSMO, with robustness test using Matlab/Simulink software.

**Keywords-** DFIG, Indirect power control (IPC), MPPT, speed observer, fuzzy sliding mode.

## 1. Introduction

wind has been among the renewable energies the highest progression , in the course of the past ten years. For WTS (wind turbine systems), the input source is variable which makes VSWTS (variable-speed wind turbine systems) more appealing than stated speed systems [1]. The DFIG has been one of the most popular machine for VSWTS applications. The DWECS result in a converter cost and power losses are lowermost with regard to a system based on a synchronous generator [2]. Moreover, we'll be able to control the statoric powers independently [3].

To optimize the sensed energy, several power control strategies have been proposed in the literature. In most of these works, the wind and rotor speeds were assumed to be available from a mechanical sensors. However, mechanical sensors increase the cost of the system and give rise to several practical problems associated with their durability, maintenance and accuracy[4].

SEC (Sensorless control) of DWECS has been obtained increasing interest in the recent years [3, 5]. The first work in speed estimation method was proposed in [6]. In [3] and [7], the authors proposed a PLL (phase lock loop) to estimate the speed and rotor position for sensorless MPPT with IPC.

Artificial intelligent techniques have proposed in a many SEC . In [2] and [8], a FLC (fuzzy logic controller) was

designed to extract the maximum aerodynamic power "fuzzy-MPPT", and in [9] a neural network estimate the wind speed, for a sensorless MPPT algorithm. In[10], MRAS (model reference adaptive system) is used for speed estimation, with a HOSMC (high-order SMC) , for extracting the maximum power. In [11], a MPPT based on mechanical torque estimation with Kalman observer associated with back-stepping control is presented. The control scheme proposed in [5] combines an HOSMO established in MPPT and a HOSMC for DFIG control. Finally, there have been two works based on FSMO, which is the approach used in this paper. In [12], the FSMO is established for an attitude heading reference system in ground vehicles, to accurately estimate the orientation even for accelerated maneuverings and magnetic disturbances. In [13], the FSMO is applied to the induction machine speed control.

In this paper, a sensorless power control strategy for a DWECS is proposed [3]. The control strategy combines a IPC and MPPT without speed subservience and FSMO for rotor flux estimation associated with rotor speed observer. The simple flux SMO proposed in [14] presents some interesting features such as robustness against modeling uncertainty, measurement noise and insensitive to parametric variations. Moreover, the discontinuous function "sign", make the sliding mode system suffer from chattering. The proposed FLC overcomes the problems of discontinuous term in the SMO and hence leads to substantial reduction of

chattering [15]. In this work, the MPPT without speed subservience is applied; the latter does not need an additional anemometer for the measurement of the wind speed [10].

This paper is divided as follows: The modeling and the control scheme of DWECS is presented in section 2. Section 3 provides the simple speed SMO. In section 4, speed FSMO is introduced. In section 5, the proposed control scheme is examined by simulation. Finally, conclusions and perspectives are given in section 6.

**2. DWECS Modeling and Control Scheme**

The proposed system is described in Fig. 1. It consisting of a WT, a gearbox, a DFIG, and two PWM converters. The DFIG is largely used for variable speed generations especially for WECS [1], and PWM converters between the rotor side and the grid side allow the power circulation in both directions.

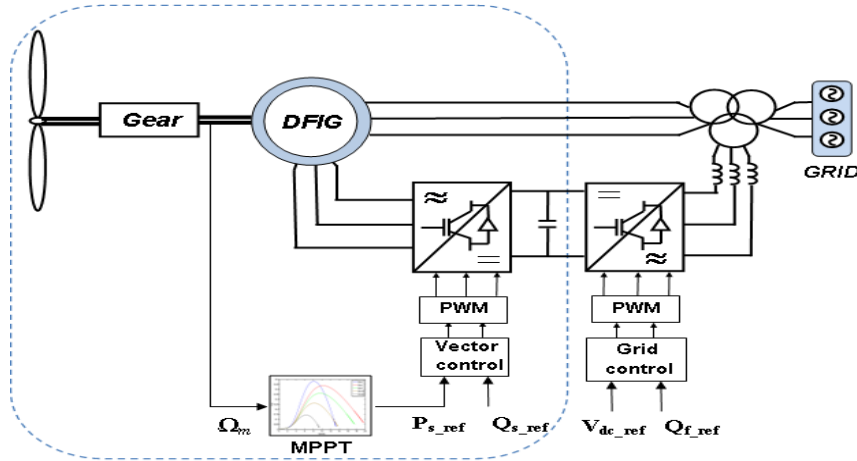


**Fig. 1.** DFIG based Wind conversion chain.

**2.1. MPPT control**

The objective of the MPPT strategy is to control the electromagnetic torque by adjusting the mechanical speed in order to maximize the generated power. In this work, the proposed MPPT control strategy does not need the wind speed measurement as shown in Fig. 2. To extract the maximum generated power, we must set the optimum speed ratio  $\lambda_{opt}$  and the maximum power coefficient  $C_{p,max}$  ( $C_{p,max} = 0.5, \lambda_{opt} = 9.2$ ) [16].

The estimate wind speed obtained from:

$$v_{est} = \frac{R \Omega_t}{\lambda_{opt}} \tag{1}$$

The reference electromagnetic torque can be expressed as follows:

$$T_{em\_ref} = \frac{1}{2} C_{p,max} \rho \pi \frac{R^5 \Omega_t^2}{\lambda_{opt}^3} \tag{2}$$

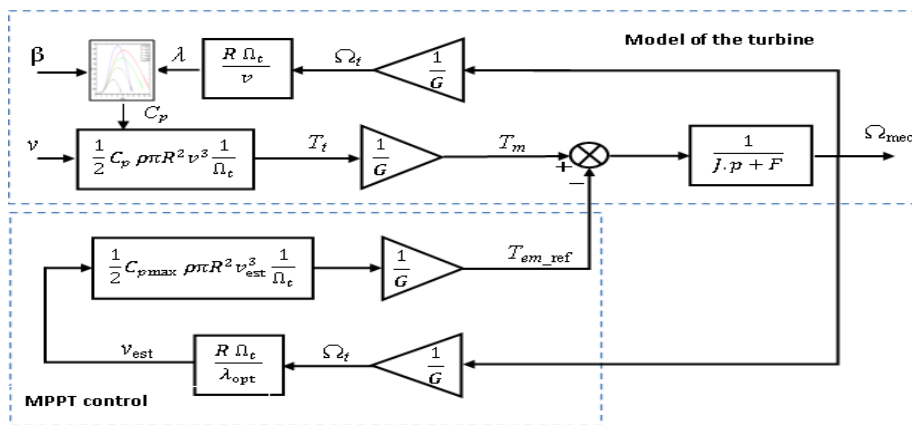


**Fig. 2.** MPPT without speed subservience.

2.2. Modeling of the DFIG

The mathematical model of the DFIG, in the (d,q) Park reference frame is described by a system of five differential equations.

$$\begin{cases} \frac{d\varphi_{sd}}{dt} = \frac{-1}{\sigma T_s} \varphi_{sd} + \omega_s \varphi_{sq} + \frac{M_{sr}}{\sigma T_s L_r} \varphi_{rd} + v_{sd} \\ \frac{d\varphi_{sq}}{dt} = \frac{-1}{\sigma T_s} \varphi_{sq} - \omega_s \varphi_{sd} + \frac{M_{sr}}{\sigma T_s L_r} \varphi_{rq} + v_{sq} \\ \frac{d\varphi_{rd}}{dt} = \frac{-1}{\sigma T_r} \varphi_{rd} + \omega_r \varphi_{rq} + \frac{M_{sr}}{\sigma T_r L_r} \varphi_{sd} + v_{rd} \\ \frac{d\varphi_{rq}}{dt} = \frac{-1}{\sigma T_r} \varphi_{rq} + \omega_r \varphi_{rd} + \frac{M_{sr}}{\sigma T_r L_r} \varphi_{sq} + v_{rq} \end{cases} \quad (3)$$

And using the equation of the torque

$$T_{em} = p \frac{1-\sigma}{\sigma M_{sr}} (\varphi_{rd} \varphi_{sq} - \varphi_{rq} \varphi_{sd}) \quad (4)$$

With:

- $R_s, R_r$  : Stator resistance , rotor resistance.
- $L_r, L_s$  : Inductance stator, Inductance rotor.
- $M_{sr}$  : Mutual inductance.
- $\sigma = 1 - M_{sr}^2 / (L_s L_r)$  : Dispersion coefficient.
- $\omega_s, \omega_r$  : Stator and rotor angular speed.
- $T_r, T_s$  : Constant stator and rotor time.

2.3. Converter control

The stator FOC has been adopted. In this work, we concentrate only on the DFIG side converter control. In the

following, it is assumed that the stator flux is oriented along d-axis . This choice is not arbitrary, but is justified by the fact that the machine is often coupled to the network with a voltage and frequency that are constant. The stator voltages and fluxes expressions can be presented:

$$\begin{cases} \varphi_{sd} = \varphi_s \\ \varphi_{sq} = 0 \end{cases} \quad (5)$$

$$\begin{cases} v_{sd} = 0 \\ v_{sq} = V_s = \omega_s \varphi_{sd} \end{cases} \quad (6)$$

The stator active and reactive powers defined by

$$\begin{cases} P_s = -\frac{V_s L_m}{L_s} i_{rq} \\ Q_s = -\frac{V_s L_m}{L_s} i_{rd} + \frac{V_s \varphi_s}{L_s} \end{cases} \quad (7)$$

From Eq. (7), it can be remarked that decoupling between the active and reactive powers is achieved with appropriate control of the currents  $i_{rd}$  and  $i_{rq}$  .The dynamic model of the DFIG is defined [16]:

$$\begin{cases} \frac{di_{rd}}{dt} = \frac{v_{rd}}{\sigma L_r} - \frac{R_r i_{rd}}{\sigma L_r} + \frac{\omega_r L_m \varphi_{sd}}{\sigma L_r L_s} + \omega_r i_{rq} - \frac{L_m}{\sigma L_r L_s} \frac{d\varphi_{sd}}{dt} \\ \frac{di_{rq}}{dt} = \frac{v_{rq}}{\sigma L_r} - \frac{R_r i_{rq}}{\sigma L_r} - \omega_r i_{rd} - \frac{L_m}{\sigma L_r L_s} \frac{d\varphi_{sq}}{dt} \end{cases} \quad (8)$$

The IPC is applied on the machine side converter, as shown in fig.3

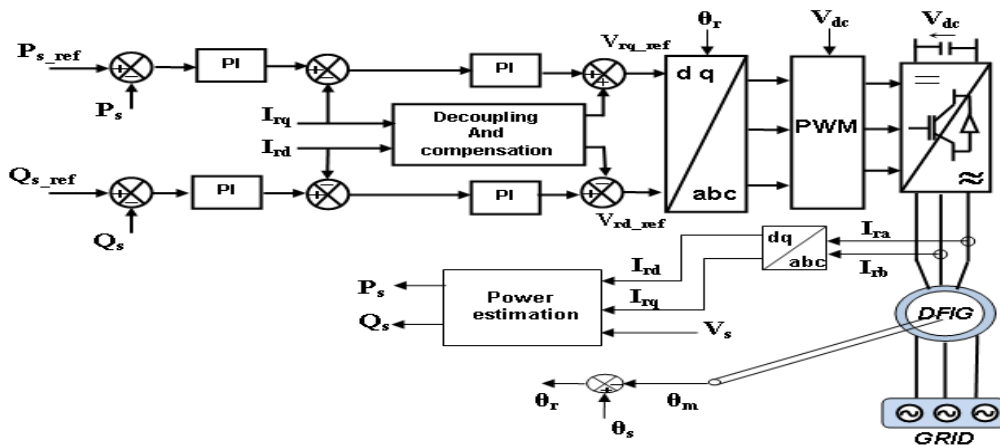


Fig. 3. DFIG Indirect power control.

**3. Speed Sliding Mode Observer**

The estimation technique used in this work is founded on SMO Fig. 4 and was proposed in [17], for speed and rotor resistance estimations. The flux SMO has been proposed for the rotor flux and stator current estimations , this is the DFIG duplicate model.

$$\begin{cases} \frac{di_{s\alpha\_e}}{dt} = -\gamma i_{s\alpha} + \frac{K}{T_r} \phi_{r\alpha\_e} + K\omega_m \phi_{r\beta\_e} + \frac{1}{\sigma L_s} v_{s\alpha} - K v_{r\alpha} + \Lambda_1 I_s \\ \frac{di_{s\beta\_e}}{dt} = -\gamma i_{s\beta} + \frac{K}{T_r} \phi_{r\beta\_e} - K\omega_m \phi_{r\alpha\_e} + \frac{1}{\sigma L_s} v_{s\beta} - K v_{r\beta} + \Lambda_2 I_s \\ \frac{d\phi_{r\alpha\_e}}{dt} = \frac{M_{sr}}{T_r} i_{s\alpha} - \frac{1}{T_r} \phi_{r\alpha\_e} - \omega_m \phi_{r\beta\_e} + v_{r\alpha} + \Lambda_3 I_s \\ \frac{d\phi_{r\beta\_e}}{dt} = \frac{M_{sr}}{T_r} i_{s\beta} - \frac{1}{T_r} \phi_{r\beta\_e} + \omega_m \phi_{r\alpha\_e} + v_{r\beta} + \Lambda_4 I_s \end{cases} \quad (9)$$

With:  $\gamma = M_{sr} / (\sigma L_s) + (R_r M_{sr}^2 / \sigma L_s L_r)$  ;  
 $K = M_{sr} / (\sigma L_s L_r)$  ;

$i_{s\alpha\_e}, \phi_{r\alpha\_e}$  :estimated values.

$\omega_m$  : angular rotor speed.

Where  $\Lambda_1, \Lambda_2, \Lambda_3$  and  $\Lambda_4$  are observer gains, with  $\Lambda_j = [\Lambda_{j1} \Lambda_{j2}]$  for  $j = 1, 2, 3, 4$ .

$I_s$  is a column vector:

$$I_s = \begin{bmatrix} \text{sign}(s_1) \\ \text{sign}(s_2) \end{bmatrix} \quad (10)$$

Where  $s_1$  and  $s_2$  are given by:

$$\begin{bmatrix} s_1 \\ s_2 \end{bmatrix} = \frac{1}{\beta} \begin{bmatrix} \frac{K}{T_r} (i_{s\alpha} - i_{s\alpha\_e}) - \omega_m K (i_{s\alpha} - i_{s\alpha\_e}) \\ \frac{K}{T_r} (i_{s\beta} - i_{s\beta\_e}) + \omega_m K (i_{s\beta} - i_{s\beta\_e}) \end{bmatrix} \quad (11)$$

$$\beta = \left[ \frac{K}{T_r} \right]^2 + K^2 \omega_m^2 \quad (12)$$

The stability of this observer was studied in [14] which have led to the following results:

$$\begin{bmatrix} \Lambda_{11} & \Lambda_{12} \\ \Lambda_{21} & \Lambda_{22} \end{bmatrix} = \begin{bmatrix} \frac{K}{T_r} \delta_1 & \omega_m K \delta_2 \\ -\omega_m K \delta_1 & \frac{K}{T_r} \delta_2 \end{bmatrix} \quad (13)$$

$$\begin{bmatrix} \Lambda_{31} & \Lambda_{32} \\ \Lambda_{41} & \Lambda_{42} \end{bmatrix} = \begin{bmatrix} \left( q_1 - \frac{1}{T_r} \right) \delta_1 & -\omega_m \delta_2 \\ \omega_m \delta_1 & \left( q_2 - \frac{1}{T_r} \right) \delta_2 \end{bmatrix} \quad (14)$$

Such as

$$\delta_1 > |e_{\phi_\alpha}|_{\max}, \delta_2 > |e_{\phi_\beta}|_{\max} \text{ And } q_1 > 0, q_2 > 0$$

The rotor speed is estimated by the adaptive scheme of Eq. (15) which represents a PI controller [17].

$$\omega_{m\_e} = k_p (e_{is\alpha} \phi_{r\beta\_e} - e_{is\beta} \phi_{r\alpha\_e}) + k_i \int (e_{is\alpha} \phi_{r\beta\_e} - e_{is\beta} \phi_{r\alpha\_e}) dt \quad (15)$$

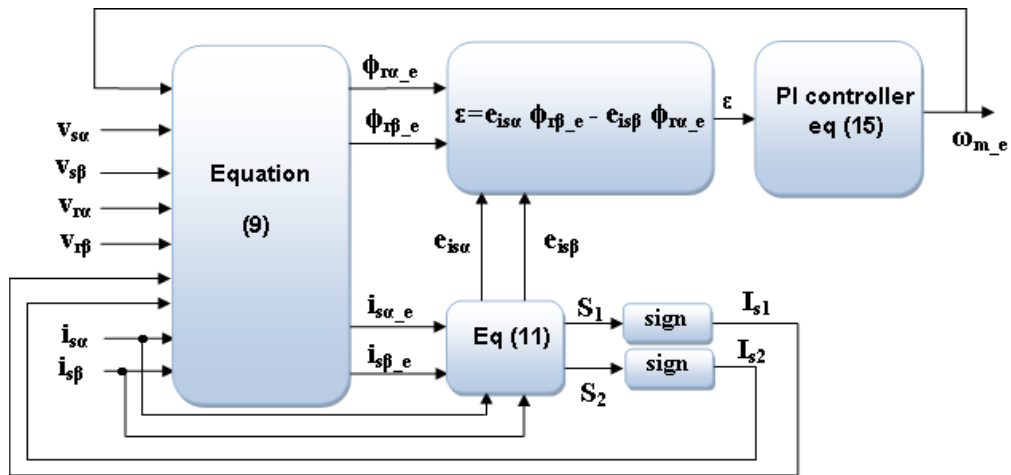


Fig. 4. Schema of Speed SMO

**4. Speed Fuzzy Sliding Mode Observer**

Chattering-free estimations may be attained using linguistic variables in place of fixed numerical values. Therefore, to improve the speed SMO efficiency, FLC is

introduced , and speed FSMO is designed. Fig. 5 shows the DWECs with the FSMO. The proposed FSMO maintains the robustness of the classical SMO and in addition reduces significantly the chattering phenomenon [12]. The FLC that replaces the "sign" function in Eq.(16).

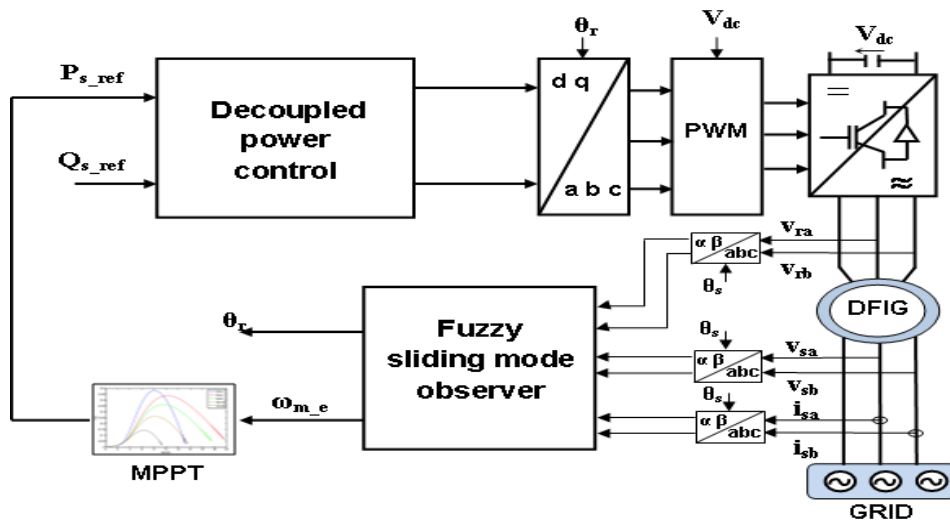


Fig. 5. Block diagram of DWECS with the speed FSMO.

$$\dot{x}_{-e} = Ax + Bu + K_s \text{sign}(y - y_{-e}) \xrightarrow{FSMO} \dot{x}_{-e} = Ax + Bu + K_s S_F \quad (16)$$

With:  $S_F = FSMO(e, \dot{e})$

The FLC inputs are the error and its derivative.

$$e(k) = i_{s\alpha\beta}(k) - i_{s\alpha\beta\_e}(k) \quad (17)$$

$$de(k) = \frac{e(k) - e(k-1)}{T_e} \quad (18)$$

Where  $T_e$  is the sampling period.

The membership functions for the error; error derivative and output are the same and are divided into seven fuzzy sets (NB, NM, NS, ZE, PS, PM, PB). The inference matrix is given in Table 1 and the membership functions are shown in Fig. 6.

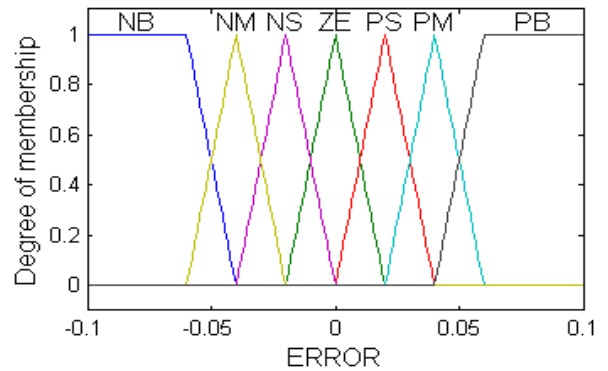


Fig. 6. Membership functions.

Table 1. Inference matrix [18].

$e$	NG	NM	NP	ZE	PP	PM	PG
$De$	NG	NM	NP	ZE	PP	PM	PG
PG	ZE	PP	PM	PG	PG	PG	PG
PM	NP	ZE	PP	PG	PG	PG	PG
PP	NM	NP	ZE	PP	PM	PG	PG
ZE	NG	NM	NP	ZE	PP	PM	PG
NP	NG	NG	NM	NP	ZE	PP	PM
NM	NG	NG	NG	NM	NP	ZE	PP
NG	NG	NG	NG	NG	NM	NP	ZE

### 5. Simulation Results and Discussions

The proposed system has been simulated using Matlab/Simulink. The DFIG and WT parameters are given in Table 2.

Table 2. Simulation parameters

Parameters	Value
<b>DFIG</b>	
Nominal power (P)	7.5 kW
rated frequency	50 Hz
Stator resistance ( $R_s$ )	0.455 $\Omega$
Rotor resistance ( $R_r$ )	0.62 $\Omega$
Stator inductance ( $L_s$ )	0.084 H
Rotor inductance ( $L_r$ )	0.081 H
Mutual inductance (M)	0.078 H
Inertia (J)	0.3125 Kg.m <sup>2</sup>
Viscous coefficient (f)	6.73*10 <sup>-3</sup> N.m.s <sup>-1</sup>
Pairs of pole number (p)	2

Wind turbine	
Nominal power	10 kW
Number of blade	3
Diameter of a blade	3 m
Multiplier Gain	5.4
inertia ( $J_r$ )	0.042 Kg.m <sup>2</sup>
Viscous coefficient ( $f_r$ )	0.017 N.m.s <sup>-1</sup>

Three simulation studies are presented, the first one is a comparative study between the two RSE (rotor speed estimation) methods "the classical SMO and FSMO" , the second is the FSMO application in the WECS control to optimize (or maximize) the DFIG active power, the last one is related to analysis the control system robustness with respect of parameter variations.

5.1. Comparative study of the proposed FSMO with the classical SMO

The tracking performance of the two methods is tested under various reference speeds and the results are shown in Fig. 7. The active power is set to "-5000 W" and the reactive power to "0 Var". The estimated speed from the FSMO has better transient response as compared to the classical SMO. From the Fig. 7 we see the difference between estimated speeds by the two observers. We notice that the chattering in FSMO estimated speed does not exist thanks to the use of the FLC.

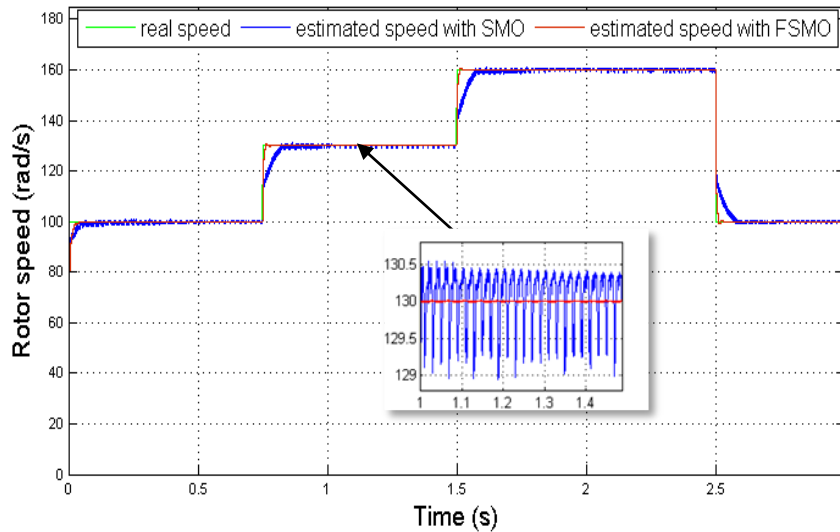


Fig. 7. Estimated speeds with SMO and FSMO.

5.2. Performance evaluation of the FSMO with the WECS.

The wind speed is modeled by Eq. (19) and the corresponding waveform is shown in Fig. 8a.

$$v(t) = 6.5 + (0.5 \sin(0.1047t) + 2 \sin(0.2665t) + \sin(1.2930t) + 0.2 \sin(3.6645t)) \quad (19)$$

Fig. 8b shows that the power coefficient  $C_p$  is around the maximum point ( $C_{p \max} = 0.5$ ) which demonstrates the effectiveness of the MPPT.

The estimated speed and real one are showed in Fig. 9a, and the estimation error in Fig. 9b with a range of [-0.06 0.06] rad/s. These results confirm that the proposed method for the RSE in real time is effective under variable wind speed conditions.

The effects of wind speed variation in the power reference is shown in Fig. 10 (a) and (b). The active and reactive power follow their respective references values with no steady state errors with fast transient responses demonstrating that the IPC is applied With a perfect decoupling.

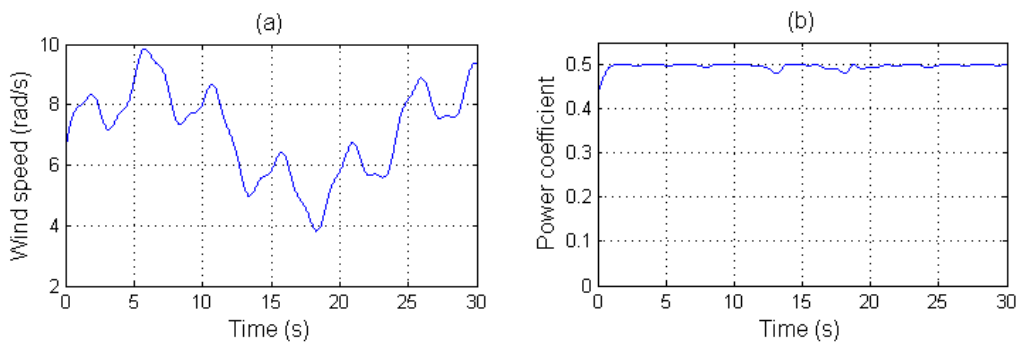


**Fig. 8.** MPPT performance (a) wind waveform (b) power coefficient ( $C_p$ )

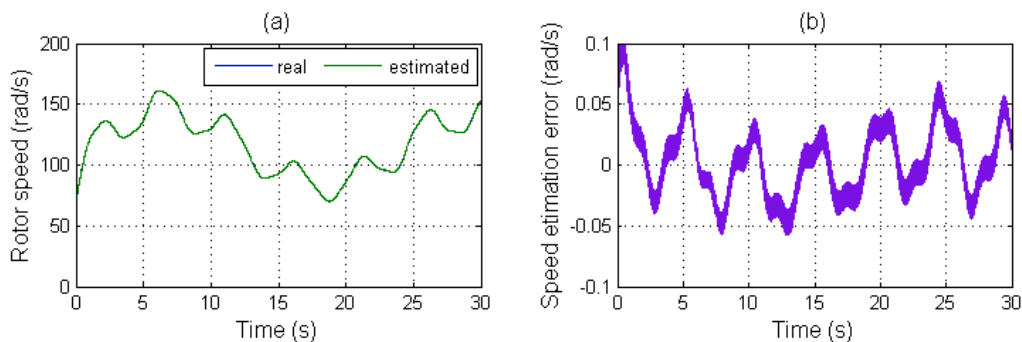


**Fig. 9.** RSE performance (a) speed tracking (b) estimation error

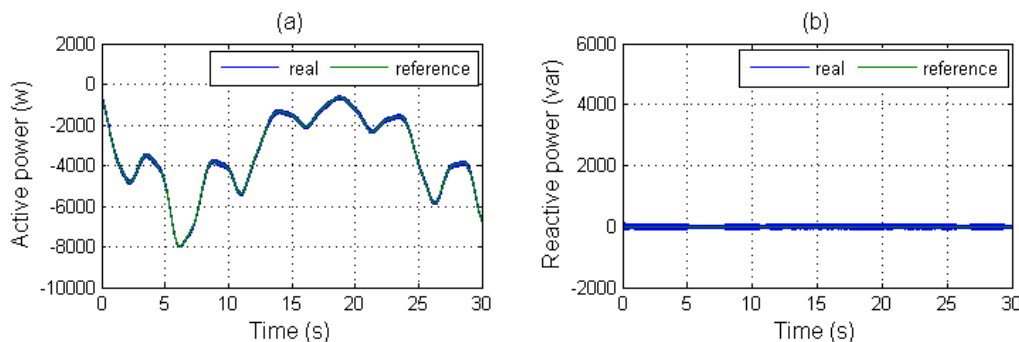


**Fig. 10.** DFIG power tracking (a) active power (b) reactive power

### 5.3. Robustness tests

The problem with estimation techniques based on a model of the machine is the sensitivity to parameter variations.

#### 5.3.1. Variation of 50% of the stator resistance

Fig. 11a shows the DFIG speed and its estimation value and Fig. 11b shows the corresponding speed tracking error, with a fork of  $[0 \ 0.3]$  rad/s. With these results we can say that

the change in the stator resistance does not have a great effect on our observer (FSMO) in the RSE.

Fig. 12a shows the response of the DFIG power and Fig. 12b represents the error between reference power in the normal condition and reference power when the variation of stator resistance (+ 50%  $R_s$ ). From Fig. 12b the error of power reference extraction is between  $[-10 \ 10]$  W. when talking about percentage it has the maximum error is 0.13% ( $\Delta P(t) / P_{ref}(t) = 10 / 8000 = 0.13\%$ ).

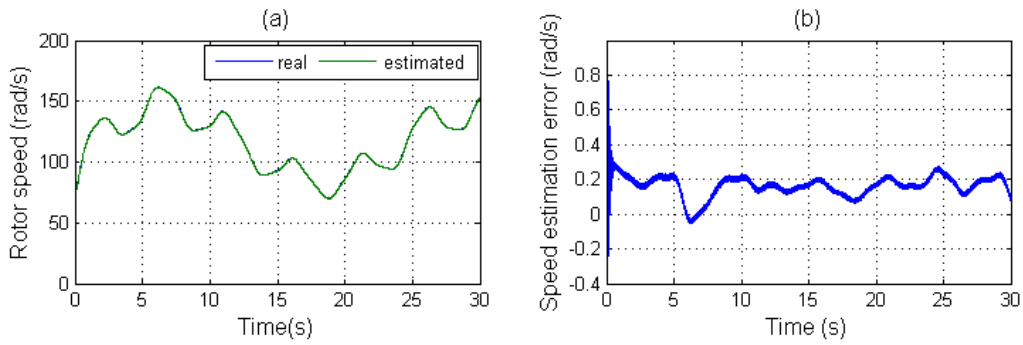


Fig. 11. RSE performance.

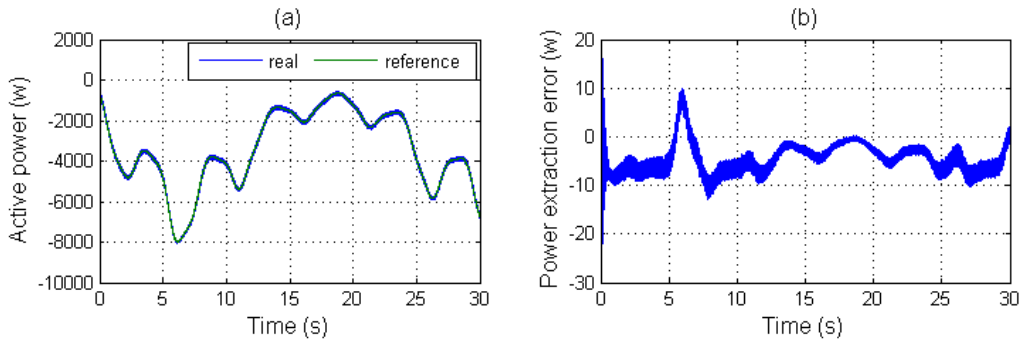


Fig. 12. DFIG power tracking (a) active power (b) power extraction error “ $P_{ref} - P_{ref}(+50\% R_s)$ ”

5.3.2. Variation of 50% of the rotor resistance

Fig. 13a shows the speed estimation with rotor resistance variation (+50%  $R_r$ ), in Fig. 13b we have a maximum speed estimation error is 3.7 (rad/s).

Fig.14 shows power extraction with rotor resistance variation (+50%  $R_r$ ), from Fig. 14b the error of power reference extraction is between [0 220] W, for power extraction under normal conditions equal to 8000 W, we have an error percentage of 2.5 % ( $220/8000 = 2.5\%$ ), this error remains in the acceptable values.

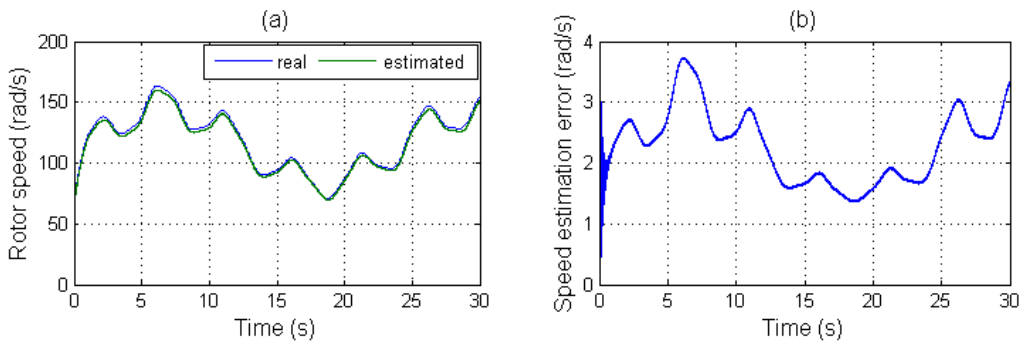


Fig. 13. RES performance.

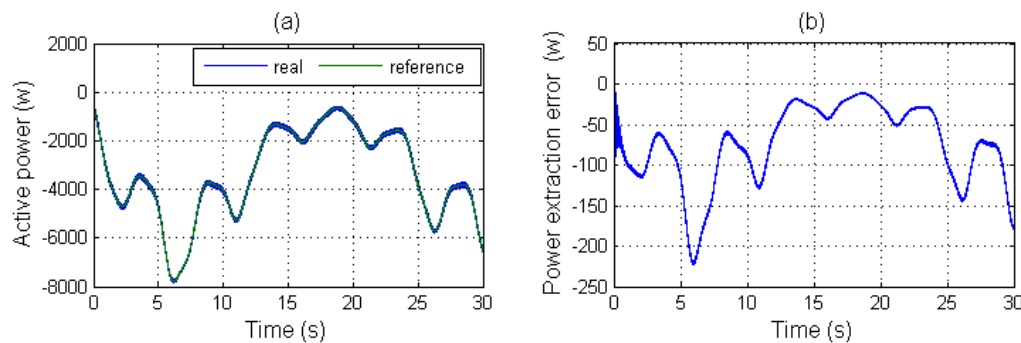


Fig. 14. DFIG power tracking (a) active power (b) power extraction error “ $P_{ref} - P_{ref}(+50\% R_r)$ ”.

## 6. Conclusion

In this paper a sensorless power optimization of DWECS using speed FSMO has been presented. The proposed control uses the FSMO to estimate the DFIG rotor speed and position, the estimated speed is used by the MPPT to extract the optimum power. The simulation results demonstrate the vantage point of FSMO compared with a classical SMO for the RSE and decreasing the chattering. Robustness tests against parametric variations developed in this work come to confirm the robustness of the our FSMO, This work can be improved in the future by employing the rotor resistance estimator to erase the error in RSE when there is a variation in rotor resistance.

## References

- [1] M. T.Abolhassani, P. Enjeti, H. A. Toliyat, "Integrated Doubly-Fed Electric Alternator/Active Filter (IDEA), a Viable Power Quality Solution, for Wind Energy Conversion Systems", *39th IAS Annual Meeting*, Seattle, pp. 2036-2043, 3-7 October 2004.
- [2] S. Abdeddaim, A. Betka, "Optimal tracking and robust power control of the DFIG wind turbine, Electrical Power and Energy Systems", *Electrical Power and Energy Systems*, Elsevier, DOI: 10.1016/j.ijepes, Vol. 49, No. 2, pp. 234-242.
- [3] F. Akel, T. Ghennam, E.M. Berkouk, M. Laour, "An improved sensorless decoupled power control scheme of grid connected variable speed wind turbine generator", *Energy Conversion and Management*, Elsevier, DOI: 10.1016/j.enconman.2013.11.015, Vol. 78, pp. 584-594.
- [4] A. Barra, H. Ouadi, "Sensorless speed and reactive power control of a dfig-wind turbine, Energy Conversion and Management", *Journal of Theoretical and Applied Information Technology*, Vol. 62, No. 2, pp. 325-334.
- [5] M.E.H. Benbouzid, B. Beltran, H. Mangel, and A. Mamoune, "A High-Order Sliding Mode Observer for Sensorless Control of DFIG-Based Wind Turbines", *IECON 2012 - 38th Annual Conference*, Montreal, pp. 4288-4292, 25-28 October 2009.
- [6] L. Xu, W. Cheng, "Torque and reactive power control of a doubly fed induction machine by position sensorless scheme", *IEEE Transactions on Industry Applications*, vol. 31, pp. 636-642, May/June 1995.
- [7] B. Shen, B. Mwinyiwiwa, Y. Zhang, and B-T. Ooi, "Sensorless Maximum Power Point Tracking of Windby DFIG Using Rotor Position Phase Lock Loop(PLL)", *IEEE Transactions on Power Electronics*, vol. 24, pp. 942-951, April 2009.
- [8] M. Bezza, B.EL. Moussaoui, A. Fakkar, "Sensorless MPPT fuzzy controller for DFIG wind turbine", *Energy Procedia*, Elsevier, DOI: 10.1016/j.egypro.2012.05.045, Vol. 18, pp. 339-348.
- [9] C. Wei, L. Qu, W. Qiao R., "Evaluation of ANN Estimation-Based MPPT Control for a DFIG Wind Turbine", *Power Electronics and Machines for Wind and Water Applications*, IEEE Symposium, Milwaukee, pp. 16, 24-26 July 2014.
- [10] K.D.E. Kerrouche, A. Mezouar, L. Boumedien, "Maximized Power Control based on High Order Sliding Mode for Sensorless DFIG Variable Speed Wind Turbine", *International Conference on Green Energy and Environmental Engineering*, Sousse, Tunisia, 2014.
- [11] T. Abd el wahed, E. Abdelmounim, M. Aboulftah, R. Majdoul, A. Moutabir, and A. elmajid, "Design of an Mppt based on the torque estimator for variable speed turbines", 1st International Conference on Electrical and Information Technologies ICEIT, Marrakech, 25-27 March 2015.
- [12] D. Keighobadi, P. Doostdar, A. Fakkar, "Fuzzy Sliding Mode Observer for Vehicular Attitude Heading Reference System", *Positioning*, vol. 4, pp. 215-226, August 2013.
- [13] C. Ben regaya, A. Zaafouri, A. Chaari, "A New Sliding Mode Speed Observer of Electric Motor Drive Based on Fuzzy-Logic", *Acta Polytechnica Hungarica*, vol. 11, pp. 219-232, 2014.
- [14] A. Benchaib, A. Rachid, E. Audrezet, "Real-Time Sliding-Mode Observer and Control of an Induction Motor", *IEEE Transactions on Industrial Electronics*, vol. 46, pp. 128-138, Feb 1999.
- [15] Y. Bekakra, "Contribution à l'Etude et à la Commande Robuste d'un Aérogénérateur Asynchrone à Double Alimentation", *PhD Thesis*, Faculty of Applied Science, Mohamed Khider University, Biskra, Algeria, 2014.
- [16] Z. Song, T. Shi, C. Xia, W. Chen, "A novel adaptive control scheme for dynamic performance improvement of DFIG-Based wind turbines", *Energy*, Elsevier, DOI:10.1016/j.energy.2011.12.029, Vol. 38, pp. 104-117.
- [17] H. Kubota, K. Matsuse, "Speed Sensorless Field-Oriented Control of Induction Motor with Rotor Resistance Adaptation", *IEEE Transactions on Industrial Applications*, vol. 30, pp. 1219-1224, Sep/Oct 1994.
- [18] A. Daoud, A. Midoun, "Commande Floue de la Charge d'une Batterie dans une Installation photovoltaïque", *Energ. Ren.: ICPWE*, pp. 67-72, 2003.